Supplement of Biogeosciences, 23, 6053–6072, 2026
https://doi.org/10.5194/bg-23-6053-2026-supplement

Biogeosciences
Open Access

Supplement of

Seasonal variations and controlling factors of nitrogen fluxes at the sediment-water interface in a semi-enclosed inland sea

Zhaosen Wu et al.

Correspondence to: Xinyu Guo (guo.xinyu.mz@ehime-u.ac.jp)

Supplementary Text

Text S1 Sensitivity analysis of the sediment model parameters

To evaluate the dependence of model results on the parameters, most parameters (Table 2) in the model—whose specific values have not been reported for the Seto Inland Sea—were individually perturbed by ±20%, and the relative sensitivity of eleven major model outputs was calculated. Figure S3 presents the results. The vertical axis represents the responses of major model outputs, including particulate organic nitrogen (PON) inventory, Ammonium (NH_4^+) inventory, nitrate (NO_3^-) inventory, nitrite (NO_2^-) inventory, dissolved oxygen (DO) inventory, PON flux, NH_4^+ flux, NO_3^- flux, and N-loss flux, while the horizontal axis lists the corresponding model parameters. Each cell reflects the magnitude of sensitivity of a given output to a specific parameter, with both the size and color of the block indicating the value of the relative sensitivity index. The sensitivity was quantified using

$$E_i = \frac{\Delta Y_j / Y_j}{\Delta X_i / X_i}$$

which represents the proportional change in output (Y_j) resulting from a proportional perturbation in the parameter (X_i).

The results indicate that the model is particularly sensitive to the sinking rate of particulate matter in the water (w_{PON}) and the critical bottom stress (τ_c). These two parameters directly affect the PON flux across the sediment–water interface. When the bottom shear stress is lower than its critical threshold, the PON flux becomes positively related to the sinking rate, leading to a nearly linear response in the sedimentary PON inventory. Since PON constitutes the dominant nitrogen pool in sediments, these parameters further extend their influence to other nitrogen species through PON mineralization. Due to the relatively low NO_3^- inventory, the NO_3^- flux and it are both particularly sensitive to these two parameters. However, the DIN flux is mainly composed of NH_4^+ flux, and 99% of TN inventory in the sediment is primarily in the form of PON. Therefore, these two parameters do not have a significant impact on the model. In addition, the parameters governing the two-step nitrification process, together with $Ks_{NO_2^-}^{Nit2}$ (Half saturation constant of NO_2^- in nitrification-step2), play an important role in controlling NO_2^- fluxes by modulating the relatively low NO_2^- inventory.

By contrast, the model exhibits relatively low sensitivity to the other parameters. For the majority of parameter–output combinations, the absolute sensitivity values are below 0.2, indicating weak or negligible influence of the change in parameters on the nitrogen dynamics in the model. Overall, the sensitivity diagram highlights that only a limited subset of parameters significantly affects the model results, while most parameters contribute minimally to output variability.

Text S2 Initial concentration of state variables and input profiles in the model

Since more than 99% of total nitrogen (TN) in sediments is PON, TN concentration profile can be set as PON initial profile[1]. The concentration of TN has its maximum value at the surface of sediment and is almost constant at 50-80 cm, which is treated as the slow-decayed PON for an exponential fitting (Figure S4a). The difference between the observed TN and the slow-decayed PON represents the fast-decayed PON.

NH_4^+ concentration, DO concentration and porosity profile are constructed by linearly interpolating the observed values (Figure S4b, d, e).

Because of the rapid reduction of NO_3^- concentration to 0 in anaerobic environment, the sum of observed NO_3^- and NO_2^- within the upper 4 cm layer are used for linear fitting as the NO_3^- concentration profile. The NO_2^- concentration profile is derived as the difference between the observed total oxidized nitrogen concentration (NO_x^-, the sum of NO_3^- and NO_2^-) and the NO_3^- concentration profile.

Text S3 Seasonal variations of bioirrigations in the sediment

Compared to the sediment–water interface fluxes, bioirrigation is negligible in magnitude. In particular, the bioirrigation of NO_3^- and NO_2^- can be safely ignored.

Bioirrigation of NH_4^+ is controlled by its sedimentary inventory, reaching a maximum in September (0.11 mmol m^{-2} d^{-1}) and a minimum in February (0.02 mmol m^{-2} d^{-1}) (Figure S5a).

NO_3^- bioirrigation exhibits a seasonal reversal in direction (Figure S5b). From January to March, NO_3^- is released from the sediment to the overlying water, with a peak value efflux in January (1 μmol m^{-2} d^{-1}). During the rest of the year, NO_3^- is transported from the bottom water into the sediment, with a maximum influx in August (4 μmol m^{-2} d^{-1}).

NO_2^- concentrations are low in both sediment and bottom water made its bioirrigation weak (Figure S5c). Its bioirrigation flux is directed into the sediment during June–September and in December, with a maximum influx in July (0.2 μmol m^{-2} d^{-1}). In other months, NO_2^- is released to the overlying water, with a peak efflux in April (0.2 μmol m^{-2} d^{-1}).

DO is consistently transported from the bottom water into the sediment via bioirrigation, with a maximum in January (0.18 mmol m^{-2} d^{-1}) and a minimum in July (0.08 mmol m^{-2} d^{-1}) (Figure S5d).

Text S4 Seasonal variations of nitrogen processes in the sediment

The seasonal variation of mineralization rate of PON in the sediment is controlled by bottom water temperature (Figure S6a). Nitrification is primarily controlled by bottom water temperature and DO concentration (Figure S6b, c). The formation and breakdown of water-column stratification regulate bottom water DO concentration, thereby influencing the DO supply to the sediment. In winter, lower temperatures suppress mineralization, allowing more DO to be preserved in the sediment and consequently promoting nitrification.

Denitrification is mainly regulated by NO_3^- availability. During summer, the influx of NO_3^- from the overlying water provides sufficient substrate to sustain denitrification (Figure S6d). Therefore, the controlling factors for denitrification are broadly consistent with those governing NO_3^- flux. Dissimilatory nitrate reduction to ammonium (DNRA) exhibits similar controls to denitrification (Figure S6e).

Anammox is primarily limited by NO_2^- availability and is thus indirectly controlled by DO (Figure S5f). Oxidation of oxygen demand units (ODU) is mainly governed by bottom-water DO concentration (Figure S6g).

Supplementary Figures

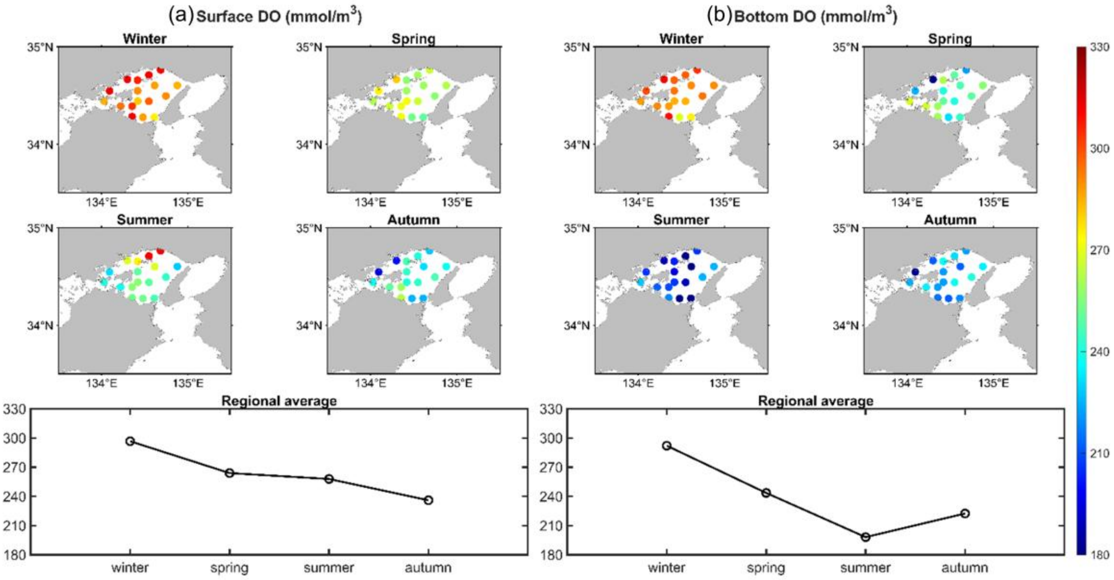

Figure S1. Seasonal spatial distributions and regionally averaged seasonal variations of dissolved oxygen (DO) concentrations (mmol/m^3) in the (a) surface and (b) bottom water column of Harima Nada in 2020.

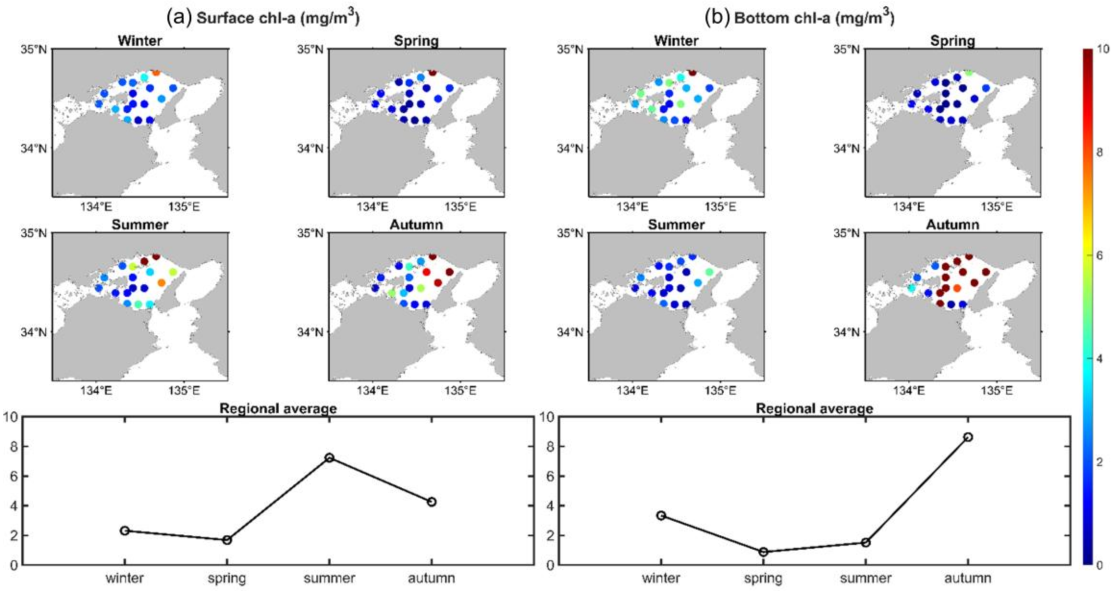

Figure S2. Seasonal spatial distributions and regionally averaged seasonal variations of Chlorophyll concentrations (mg/m^3) in the (a) surface and (b) bottom water column of Harima Nada in 2020.

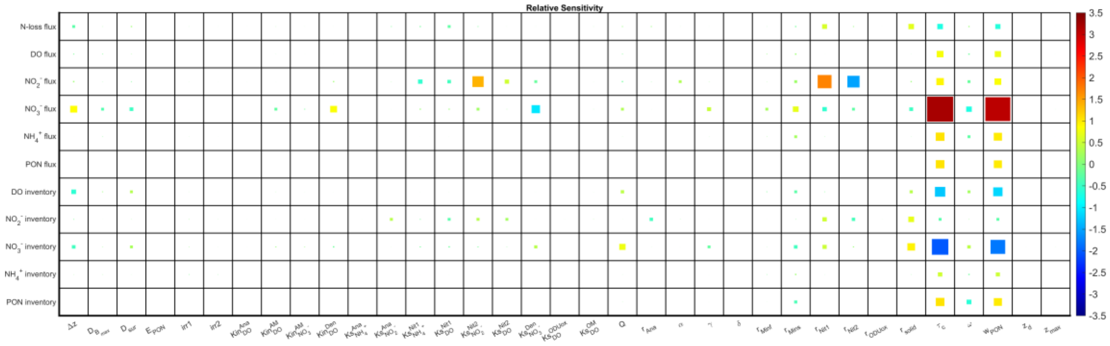

Figure S3. Sensitivity Analysis. The percentage change in the annual average of the main results when the parameter changes by 1%. The expression for relative sensitivity ($\boldsymbol{E_{ij}}$) is $\boldsymbol{E_{ij}} = \frac{\Delta Y_j/Y_j}{\Delta X_i/X_i}$, where $\boldsymbol{Y_j}$ represents the model results given along the y-axis, $\boldsymbol{X_i}$ represents the parameters along the x-axis, and $\boldsymbol{E_{ij}}$ is represented by the colour and size of the block inside the grid corresponding to $\boldsymbol{X_i}$ and $\boldsymbol{Y_j}$. No colour indicates that $\boldsymbol{E_{ij}}$ is too small and can't be exhibited.

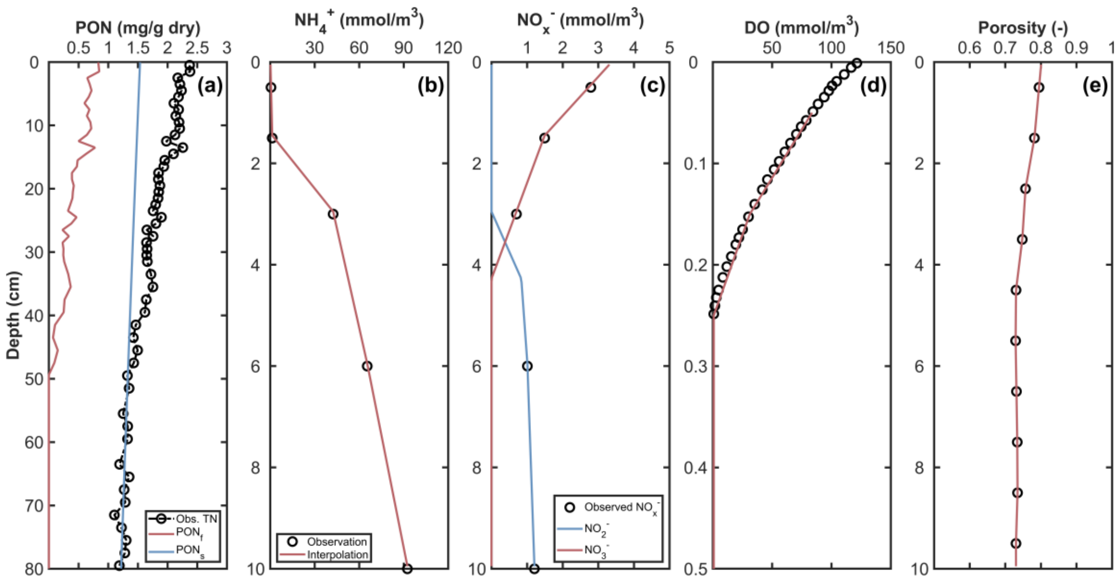

Figure S4. Initial and input profiles for the sediment model: (a) PON; (b) $\mathbf{NH_4^+}$; (c) $\mathbf{NO_3^-}$ and $\mathbf{NO_2^-}$; (d) DO; (e) porosity.

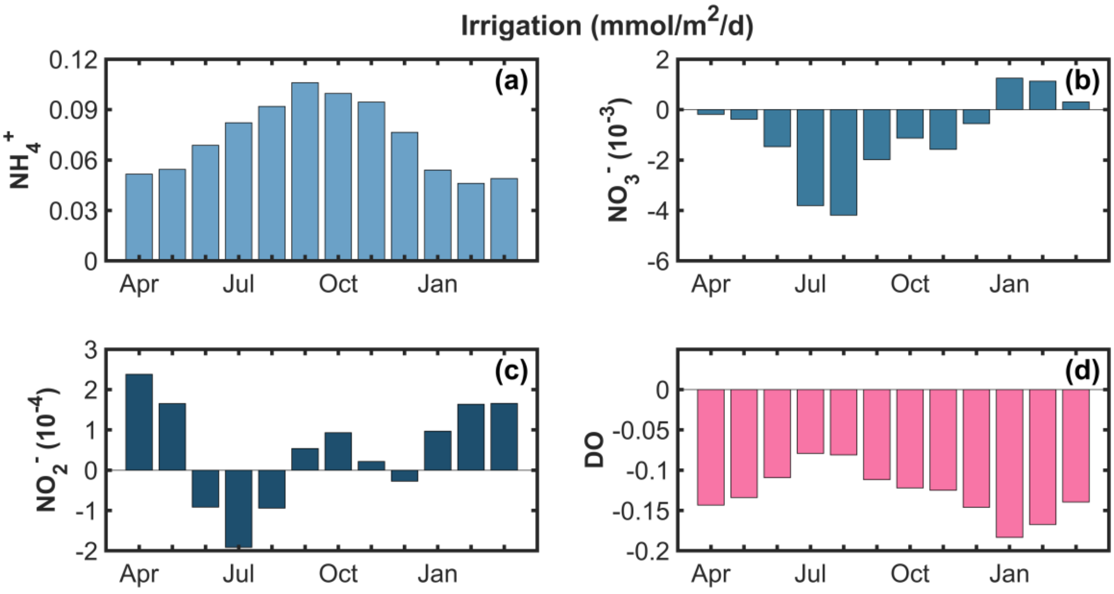

Figure S5. The seasonal variations of bioirrigations of (a) $\mathbf{NH_4^+}$, (b) $\mathbf{NO_3^-}$, (c) $\mathbf{NO_2^-}$ and (d) DO in the sediment.

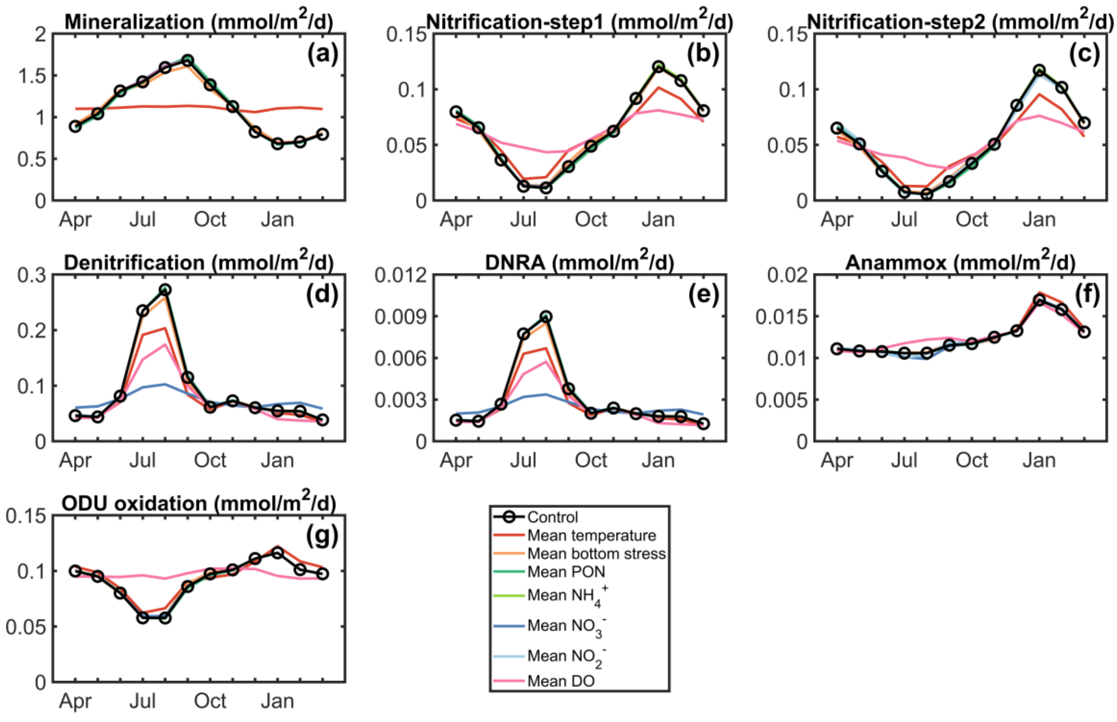

Figure S6. Seasonal variations and the controlled factors of nitrogen reaction rates in the sediment: (a) mineralization; (b) nitrification (step 1); (c) nitrification (step 2); (d) denitrification; (e) DNRA; (f) anammox; (g) ODU oxidation. The lines with different colors represent model results of the sensitivity experiments for seasonal variations.

References

1. Nakakuni, M.; Yamaguchi, H.; Ichimi, K.; Tada, K., Seasonal variation in pore water nutrients and their fluxes from the bottom sediments in Harima Nada, Seto Inland Sea. *Journal of Oceanography* **2024,** *80*, (3), 219-232.